Energy Proceedings
Vol 43, 2024
ISSN 2004-2965

Numerical Analysis on Conceptual Feasibility of Hybrid Windcatcher and Turbine Roof Ventilator for Optimum IEQ and Wind Power Harvesting

Diana SNM Nasir [1*], Ben Richard Hughes [2], Azlizawati Ibrahim [3]

1 Department of Mechanical Engineering, School of Engineering, Faculty of Science and Engineering, University of Hull, UK

(*Corresponding Author: D.Mohd-Nasir@hull.ac.uk)

2 The Energy Institute, The University of Sheffield, UK

3 Edinburgh School of Architecture and Landscape Architecture (ESALA), University of Edinburgh, UK

ABSTRACT

This paper introduces "SmartTURVENT," a hybrid windcatcher and turbine roof ventilator system with triple benefits: enhancing indoor environmental quality (IEQ), harnessing renewable energy, and reducing carbon emissions. Utilising a transient state pressure-based solver with CFD airflow modeling, the SmartTURVENT system optimises heat exchange, achieving about 6-40% and 11-55% faster attainment of acceptable humidity levels compared to individual windcatcher and turbine roof ventilator operations, respectively. In energy harvesting, SmartTURVENT generates 0.37 W, 11.27 W, and 69.10 W at wind speeds of 2 m/s, 5 m/s, and 10 m/s, respectively. Over an 8-hour operation, SmartTURVENT reduces carbon emissions by an average of 13.0% compared to conventional systems.

Keywords: Indoor environmental quality, dynamic mesh modelling, computer fluid dynamics (CFD), thermal airflow modelling, thermal comfort, carbon emission reduction.

NONMENCLATURE

Abbreviations

SmartTURVENT	Smart hybrid turbine roof ventilator and windcatcher system
COVID-19	Coronavirus disease 2019
IEQ	Indoor environmental quality
UN SDG	United Nation Sustainable Development Goal
VAWT	Vertical axial wind turbine
RPM	Revolution per minute

Symbols

A	Sum surface area calculated based on the model's building fabric, m^2
A_G	Sunlight area of the glazing, m^2
A_T	Total surface area involved, of 103.0 m^2
Cv	Specific heat capacity of an indoor air, to be set as 1006 J/m^3K
E_{HG}	Equipment heat gain of 10 W/m^2
GF_S	Solar gain factor (unitless) as referred to CIBSE Guide A for UK office
HL_F	Total heat losses through building fabric in sigma, W
HL_v	Total heat losses through ventilation and air filtration, W
L_{HG}	Lighting heat gain of 12 W/m^2
N	Number of complete air changes per hour, ACH
P_{LHG}	Latent heat gain/person of 3 W/m^2
P_{SHG}	Sensible heat gain/person of 4 W/m^2 for an executive officer
P_T	Total power output generated based on torque force, W
Q_C	Heat exchange between building fabric and structures, W
Q_I	Internal heat gain (W) from the space through activities carrying in the space
Q_L	Heat loss from the space, W
Q_S	Solar heat gain (W) based on solar intensity via sun glazing and gain factor

This is a paper for 15th International Conference on Applied Energy (ICAE2023), Dec. 3-7, 2023, Doha, Qatar.

r	Radius of the blade, m
S_I	Mean solar intensity (W/m^2) for Hull city of UK, of 94.875 W/m^2
ΔT	Indoor-outdoor temperature variance, °C
T_F	Estimated torque force based on moment of force, Nm
U_T	Average thermal transmittance of overall model wall surfaces, of 0.8 W/m^{2}K
V	Volume of the model's room, m^3
V_{Tan}	Tangential velocity, m/s
ω	Angular speed, rad/s

1. INTRODUCTION

The COVID-19 pandemic has heightened the importance of effective indoor ventilation, particularly in high-occupancy spaces [1]. Meeting new ventilation standards amidst energy efficiency concerns necessitates a focus on innovative technologies, especially those optimising natural ventilation using rooftop elements. Leveraging principles like the Venturi effect and Bernoulli's principle enhances the efficiency of buoyancy-driven natural ventilation by inducing temperature and pressure differences along the roof area [2]. Inspired by traditional methods, modern roof ventilators and windcatchers apply these techniques on a compact scale. Exploring renewable potential from small-scale technologies aligns with UN SDG Goal 7 for Affordable and Clean Energy, aiming for carbon reduction by 2030 and 2050. Turbine roof ventilators, resembling VAWT systems, provide fresh air through passive, active, or hybrid wind-driven techniques. The rotor, driven by external high winds, creates an updraft inside the turbine. Roof ventilator dimensions range from 300-600 mm inner diameter to a reported 1000 mm external diameter, tested at wind speeds of 1-15 m/s [3]. Effective natural ventilation requires open areas for airflow, and integrating turbine ventilators with other devices is suggested for improved ventilation, energy efficiency, and IEQ [4]. In hot, humid climates, a hybrid approach with multiple roof ventilators is recommended for efficient heat exhaust from roof attics [5]. Therefore, the aim of this research was to evaluate on the conceptual feasibility of SmartTURVENT involving the hybrid of two wind-driven ventilation technologies. Three objectives were achieved under the aim, as below:

1) To conduct an airflow thermal analysis of SmartTURVENT system to evaluate its performance in terms of indoor comfort with the setting of several operations of SmartTURVENT in the influence of wind speed and ambient condition (indoor-outdoor);

2) To obtain the power output of the rotated SmartTURVENT's turbine blade based on Objective 1;

3) To estimate the performance of SmartTURVENT in minimising the carbon emission based on a case of operating a space/room based on Objective 2.

2. CFD THERMAL AIRFLOW MODELLING

2.1 Design configuration

SmartTURVENT features are configured in two separate zones by adding a compartment which disintegrates the incoming air (VENTCatcher) and the exhaust air (VENTurbine) positions, as depicted in Figure 1. Table 1 provides the details of the components, number of units, properties, materials, and size which determined the design configuration of SmartTURVENT.

2.2 ANSYS DesignModeler and Mesh

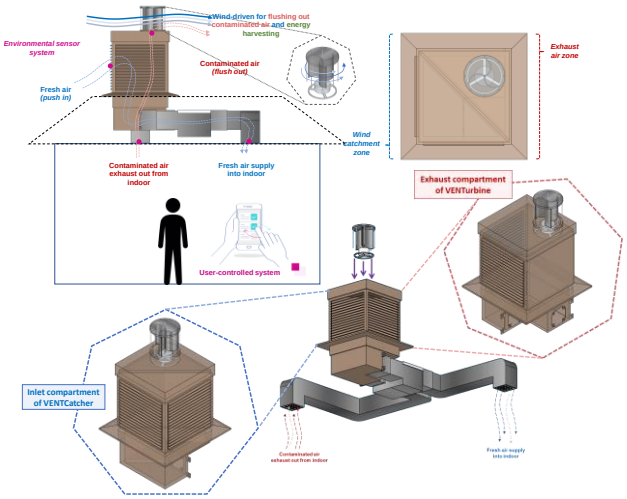

Fig. 1. Conceptual diagram of SmartTURVENT

The SmartTURVENT CAD model was used to create two flow domains, as depicted in Figure 2. The first, termed the "macro flow domain", combines the SmartTURVENT CAD geometry with external and internal fluid bodies representing outdoor and indoor environments, respectively. Fine mesh elements were applied in priority contact regions near air intake and exhaust air zones, with automatic larger elements in distant areas. The second type, the "micro flow domain", includes various fluid bodies and a 3-blade half-moon Savonius VAWT turbine (VENTurbine). Torque force, tangential velocity, and angular velocity of the VENTurbine blade were estimated under constant wind speed. Averaged outputs per second were then set as

boundary values for VENTurbine rotational speed in the macro flow domain.

Table 1. Details on SmartTURVENT 3D CAD geometry

Component	Unit	Properties	Material	Dimension / volume
1) VENTCatcher			Aluminium	1.0716 m^3
- wind catchment	1	Fluid zone	(outer body)	1.0843 m^3
- louvres (on/off)	32	Diameter = 8.9 mm 895 mm (W) × 53 mm (H)		1.602 m^2
- incoming air ducting	1	Fluid zone		4.1412 m (L)
2) VENTurbine				1.215 m^3
- 3-blade half-moon Savonius VAWT type	1	r = 200 mm Thickness = 10 mm Height = 300 mm Mass = 2.59 kg Density = 930kg/m^3	PLA	0.0027834 m^3
- exhaust air zone	1	Fluid zone	Aluminium	1.0843 m^3
- exhaust air ducting	1		(outer body)	4.1412 m

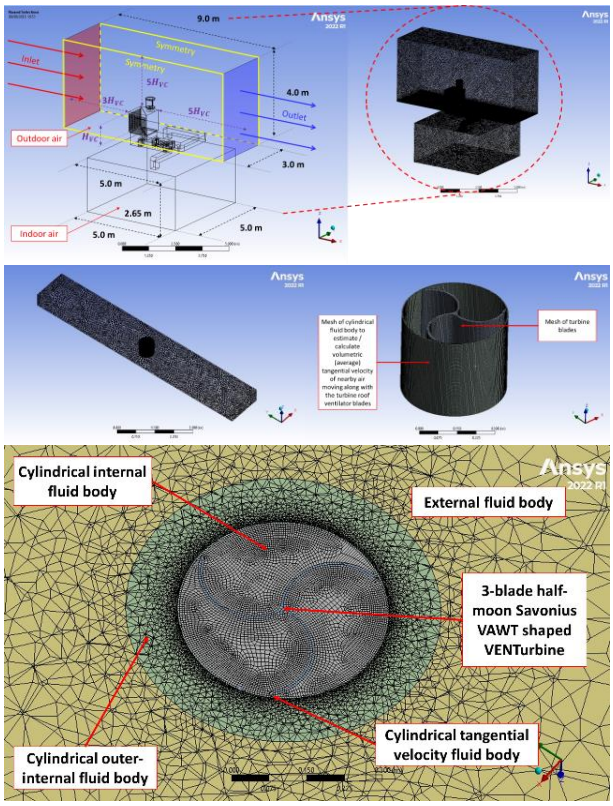

Fig. 2. Mesh of macro and micro flow domains

2.3 Computational governing equations

ANSYS Fluent 2022 R1 was employed to run the CFD simulation on both domains using transient state pressure-based solver with Energy model, Species Transport model and Realizable K-Epsilon (k-ε) viscosity model (enabling Enhanced Wall Treatment and Pressure Gradient Effect options). Realizable K-Epsilon model was selected due to the model can provide a stable performance of the fluid flow dealing with rotation, recirculation, and boundary layer. Transient state time allows to record the changes over a set of time, while Enhanced Wall Treatment with Pressure Gradient Effect options will improve the accuracy of near wall modelling approach and refine the meshes without degrading the results of the wall function meshes.

2.4 Boundary conditions

Two investigations, Study 1 and 2, were performed with specified parameters and boundary settings. Initially, a pre-study on the spinning effects of the 3-blade half-moon Savonius VAWT-shaped VENTurbine was conducted in the micro flow domain. This involved three wind speed settings (2 m/s, 5 m/s, and 10 m/s), with the Energy model turned off to eliminate thermal effects. ANSYS Fluent's "Smooth" dynamic mesh method with Six DOF option facilitated blade rotation. Rotational effects influenced the cylindrical tangential velocity fluid region, and the VENTurbine blade wall reported the moment of force (N·m). The cylindrical tangential velocity fluid region reported volume-average tangential velocity in 1000-time steps or 20,000 iterations. The average tangential velocity in m/s was converted to an average angular velocity in rad/s. This value was then applied under the Boundary Condition tab for the rotation wall representing the VENTurbine blade in the macro flow domain.

2.4.1 Setting for Study 1

For Study 1, three conditions of outdoor air and indoor air were set as the boundary settings, annotated as SETTING A, SETTING B, and SETTING C. The parameters required for these settings are described under Table 2. Study 1 investigated on the performance of SmartTURVENT under various indoor and outdoor conditions comparing i) OPERATION I: only VENTCatcher to operate, ii) OPERATION II: only VENTurbine to operate, and iii) OPERATION III: VENTCatcher and VENTurbine to operate simultaneously.

2.4.2 Setting for Study 2

In Study 2, power output and carbon savings from the rotational speed of the VENTurbine blade were acquired through the SmartTURVENT simulation using MathWorks® MATLAB Simulink R2022a. The emitted carbon, calculated from the SmartTURVENT's power output, was compared with conventional energy operation. This assessment included the energy balance equation (Equation 1) considering the heat/cool supply needs for building interiors.

$$Q_E = Q_L - (Q_S + Q_I + Q_C) \quad \text{(Eq.1)}$$

Table 2. Boundary condition for Study 1

Parameter	Description	Value	Unit
Outdoor air condition	To evaluate the influence of outdoor air condition as follows on indoor thermal condition		
	• Wind speed	2, 5, 10	m/s
	a) Turbulent length scale, *l*	0.24	m
	b) Reynolds number, *Re*	2 m/s = 26,825	-
	c) Turbulent intensity, *I*	5 m/s = 67,062	-
		10 m/s = 134,123	-
		2 m/s = 0.04476	%
		5 m/s = 0.03989	%
		10 m/s = 0.03657	%
	• Air temperature	Setting A = 20.0	°C
		Setting B = 20.0	°C
		Setting C = 15.0	°C
	• Relative humidity	All settings = 40.0	%
	• H_2O mass fraction	A & B = 0.00576	kg/kg
		C = 0.0042	kg/kg
	• O_2 mass fraction	A & B = 0.22867	kg/kg
		C = 0.22903	kg/kg
Initial indoor ambient condition	To set an initial indoor air temperature representing summer days without using any mechanically operated ventilation or air-conditioning		
	• Air temperature	Setting A = 30.0	°C
		Setting B = 35.0	°C
		Setting C = 35.0	°C
	• Relative humidity	All settings = 60.0	%
	• H_2O mass fraction	A = 0.01579	kg/kg
		B & C = 0.02099	kg/kg
	• O_2 mass fraction	A = 0.22637	kg/kg
		B & C = 0.22517	kg/kg
Incoming air supply from VENTCatcher	To set the turn on and off operation • Turn on for OPERATION A & C • Turn off for OPERATION B	When turn off: The gaps between louvres were removed by adding walls to prohibit air penetration	
Exhaust air out from VENTurbine	To set the turn on and off operation • Turn on for OPERATION B & C • Turn off for OPERATION A	When turn on: The rotational speed (rad/s) input values were based on volume-average tangential velocity obtained from micro flow domain simulation results	

The estimated power generated from VENTurbine depends on the estimated torque force of the blade, angular velocity, and tangential velocity of the nearby air moving along with the blade; as Equation 2 and 3 below:

$$P_T = T_F \times \omega \quad \text{(Eq.2)}$$

$$\omega = V_{Tan} \times r \quad \text{(Eq.3)}$$

Based on Equation 1, the Q_L, Q_S, Q_I and Q_C were expanded based on Equation 4-9. All these equations and values were referred to CIBSE Guide A: Environmental Design and UK Building Regulation Approved Document L.

$$Q_L = HL_v + HL_F \quad \text{(Eq.4)}$$

$$HL_v = \frac{Cv \times N \times V \times \Delta T}{3600\ s} \quad \text{(Eq.5)}$$

$$HL_F = \sum A \times U \times \Delta T \quad \text{(Eq.6)}$$

$$Q_S = S_I \times A_G \times GF_S \quad \text{(Eq.7)}$$

$$Q_I = P_{SHG} + P_{LHG} + E_{HG} + L_{HG} \quad \text{(Eq.8)}$$

$$Q_C = U_T \times A_T \times \Delta T \quad \text{(Eq.9)}$$

The estimated value of carbon impact comparing with and without the power harvested from SmartTURVENT system was then obtained based on Equation 10. It should be noted that $P_{SmartTURVENT}$ is the generated power output of SmartTURVENT while $CO_{2(EF)}$ is the carbon emission factor.

$$CE = P_{SmartTURVENT} \times \frac{1}{1000} \times CO_{2(EF)} \quad \text{(Eq.10)}$$

3. RESULTS AND DISCUSSION

3.1 Obtaining angular speed of VENTurbine blade

From micro flow domain simulations, the VENTurbine blade's average angular and rotational speeds were determined using Equations 3 and 4. At wind speeds of 2 m/s, 5 m/s, and 10 m/s, the blade exhibited angular speeds of 0.7459 rad/s, 2.9338 rad/s, and 3.7655 rad/s, respectively. This indicates a proportional increase in rotational speed with higher wind speeds. Additionally, the average moment of force on the blade increased with wind speeds, measuring 0.49 N·m, 3.84 N·m, and 18.35 N·m, respectively. However, a comparison with previous works [3] revealed that the obtained RPM of the SmartTURVENT turbine blade were notably low, registering only 7.12 RPM, 28.02 RPM, and 36.75 RPM at wind speeds of 2 m/s, 5 m/s, and 10 m/s, respectively.

3.2 Study 1: Analysis on indoor thermal condition in various SmartTURVENT operations and wind speed

Figures 3(a), 3(b) and 3(c) illustrate the temperature contours of an indoor space under SmartTURVENT OPERATION I, II, and III, respectively, tested at wind speeds of 2 m/s, 5 m/s, and 10 m/s over a 15-minute period. Simulation results reveal that the hybrid operation of VENTCatcher and VENTurbine significantly expedites heat exchange within the indoor space, achieving comfort conditions (19.0 °C ~ 23.0 °C) faster than individual operations. At a low wind speed of 2 m/s, the hybrid system achieved comfort in 15 minutes under SETTING C, while SETTING A and SETTING B took over 20 minutes. At 5 m/s, the hybrid system achieved comfort in 2 minutes, 3.25 minutes, and 13 minutes for SETTING C, SETTING B, and SETTING A, respectively.

Under SETTING B, comfort was sustained beyond 5 minutes due to a temperature equilibrium. At 10 m/s, the single VENTCatcher operation matched some hybrid performance, achieving comfort in less than 10 minutes. The hybrid system under 10 m/s performed fastest, reaching comfort within 2.5, 3, and 11.5 minutes for SETTING C, SETTING A, and SETTING B, respectively. However, in SETTING C, comfort only sustained for 4 minutes before a temperature drop, while SETTING A sustained comfort after 15 minutes. For SETTING B, the

temperature equilibrium took over 20 minutes due to a higher initial indoor ambient temperature. Figure 4 presents a 20-minute plot of indoor ambient temperature versus temperature reduction, comparing three SmartTURVENT operational settings: 1) OPERATION I, 2) OPERATION II, and 3) OPERATION III.

3.3 Study 2: Estimated power output from rotational force and carbon saving

3.3.1 Power harvesting from VENTurbine blade

The Simulink model estimated that, at this conceptual stage, the SmartTURVENT system generates 0.37 W, 11.27 W, and 69.10 W at wind speeds of 2 m/s, 5 m/s, and 10 m/s, respectively. This half-moon VAWT shape with a 400 mm diameter and 300 mm height was observed obtaining lower angular speed than expected based on the previous works [3].

3.3.2 Carbon saving of SmartTURVENT operations

Based on Equations 1-10 as configured in our Simulink model, total carbon dioxide (CO2) emissions were estimated by comparing those from a conventional energy-operated indoor office room to emissions from a room incorporating the SmartTURVENT system. Table 2 compares total carbon emissions between simulated data using conventional energy and conditions with a small amount of power harvested from SmartTURVENT. Simulating an 8-hour occupancy during the summertime in Hull, UK, with solar irradiance according to its climate, we presumed SmartTURVENT was operated for 8 hours. Multiplying the power output from our CFD simulation,

Table 3. Carbon saving of SmartTURVENT

Parameter	Total CO_2 emission from 8-hour room operation incorporating SmartTURVENT system ($kgCO_2e$)	Carbon saving based on proposed system (%)
Total CO2 emission from 8h room operation using conventional electricity system: ΔT = 10.0 °C (need heating) = 0.2477 kgCO2e ΔT = 15.0 °C (need cooling) = 0.2903 kgCO2e ΔT = 20.0 °C (need cooling) = 0.8283 kgCO2e		
With 0.37 Wh (from 2 m/s): 8 hours operation = 2.96 Wh		
ΔT = 10.0 °C (need heating)	0.2471	0.24 %
ΔT = 15.0 °C (need cooling)	0.2896	0.24 %
ΔT = 20.0 °C (need cooling)	0.8276	0.08 %
With 11.27 Wh (from 5 m/s): 8 hours operation = 90.16 Wh		
ΔT = 10.0 °C (need heating)	0.2286	7.71 %
ΔT = 15.0 °C (need cooling)	0.2711	6.61 %
ΔT = 20.0 °C (need cooling)	0.8091	2.32 %
With 69.1 Wh (from 10 m/s): 8 hours operation = 552.8 Wh		
ΔT = 10.0 °C (need heating)	0.1303	47.40 %
ΔT = 15.0 °C (need cooling)	0.1729	40.44 %
ΔT = 20.0 °C (need cooling)	0.7109	11.74 %

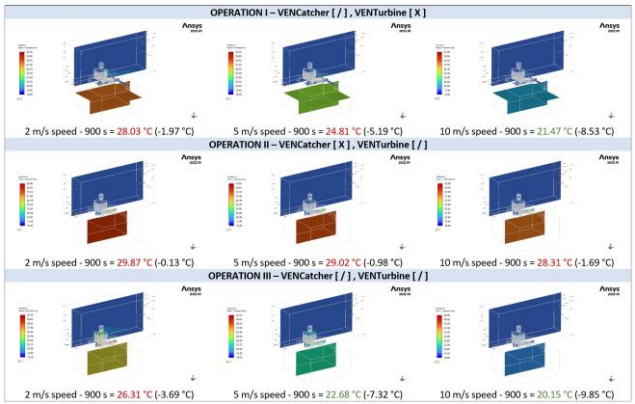

(a) SETTING A (Outdoor = 30.0 °C, Indoor = 20.0 °C)

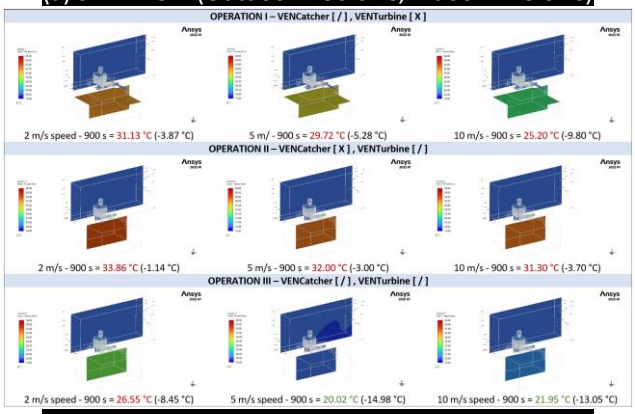

(b) SETTING B (Outdoor = 35.0 °C, Indoor = 20.0 °C)

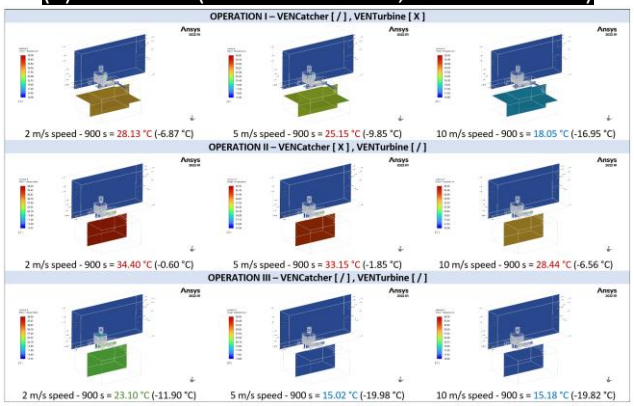

(c) SETTING C (Outdoor = 35.0 °C, Indoor = 15.0 °C)

Fig. 3. Indoor temperature influenced by OPERATION I-III according to SETTING A-C at 900 s period. Note that: Red = too warm, green = comfortable, blue = too cold

set at 2 m/s, 5 m/s, and 10 m/s wind speeds, by yielded an 8-hour stored power, assuming near-constant wind speed. CO2 emission factor of 0.21233 kgCO2e/kWh from the UK government (2021) was adopted. As in Table 3, heightened power output reduces carbon emissions, but the increased heating/cooling loads may offset savings. This aligns with the UN agenda, stressing the need for a system to maintain or surpass the harvesting performance. The shift from a 15.0 °C to 20.0 °C

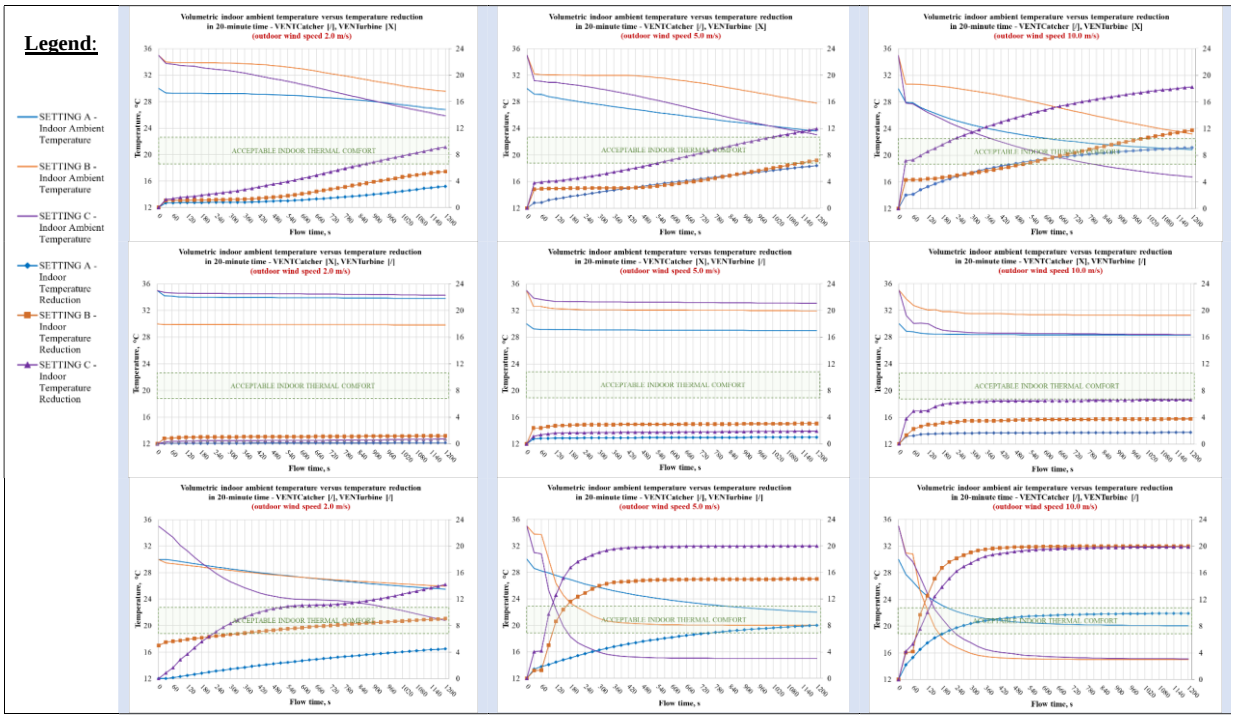

Fig. 4. 20-minute plot of indoor ambient temperature versus temperature reduction comparing different operations

temperature difference led to substantial reductions in carbon savings at wind speeds of 2 m/s, 5 m/s, and 10 m/s by 67.0%, 65.0%, and 71.0%, respectively.

4. CONCLUSIONS

In our SmartTURVENT concept, the Savonius VAWT VENTurbine blade, with a 200 mm radius and 300 mm height, achieved tangential velocities from 2 to 3.77 rad/s at outdoor wind speeds of 2 m/s to 10 m/s. The hybrid VENTCatcher and VENTurbine operation increased indoor-outdoor temperature exchange by 6-55% compared to individual operations. Optimal performance occurred at 2-3.25 minutes for 5 m/s wind, with a maximum of 12 minutes. At 10 m/s wind, the hybrid operation mirrored the 5 m/s performance, sustaining comfort for 2.5-11.5 minutes. Simulated angular speed and torque resulted in estimated power outputs of 0.37-69.10 W, showcasing SmartTURVENT's average carbon saving capability by 13.0%.

ACKNOWLEDGEMENT

This work was supported by the University of Hull under 2022/23 Research and Impact Staff Support Fund (RISSF) of GBP 3,845.00 awarded to Dr Diana Mohd Nasir.

DECLARATION OF INTEREST STATEMENT

The authors declare that they have no known competing financial interests or personal relationships that could have appeared to influence the work reported in this paper. All authors read and approved the final manuscript.

REFERENCE

[1] T. T. Moghadam, C. E. Ochoa Morales, M. J. Lopez Zambrano, K. Bruton, and D. T. J. O'Sullivan, "Energy efficient ventilation and indoor air quality in the context of COVID-19 - A systematic review," Renewable and Sustainable Energy Reviews, vol. 182. Elsevier Ltd, Aug. 01, 2023. doi: 10.1016/j.rser.2023.113356.

[2] T. F. Ishugah, Y. Li, R. Z. Wang, and J. K. Kiplagat, "Advances in wind energy resource exploitation in urban environment: A review," Renewable and Sustainable Energy Reviews, vol. 37, pp. 613–626, Sep. 2014, doi: 10.1016/J.RSER.2014.05.053.

[3] H. Zhang et al., "A critical review of combined natural ventilation techniques in sustainable buildings," Renewable and Sustainable Energy Reviews, vol. 141, p. 110795, May 2021, doi: 10.1016/J.RSER.2021.110795.

[4] J. H. Park, M. H. Chung, and J. C. Park, "Development of a small wind power system with an integrated exhaust air duct in high-rise residential buildings," Energy Build, vol. 122, pp. 202–210, Jun. 2016, doi: 10.1016/J.ENBUILD.2016.04.037.

[5] K. M. Al-Obaidi, M. Ismail, and A. M. Abdul Rahman, "Design and performance of a novel innovative roofing system for tropical landed houses," Energy Convers Manag, vol. 85, pp. 488–504, Sep. 2014, doi: 10.1016/J.ENCONMAN.2014.05.101.